Journal of Hydrology

Groundwater hydrochemistry in the active layer of the proglacial zone, Finsterwalderbreen, Svalbard

R.J. Cooper[a], J.L. Wadham[a,*], M. Tranter[a], R. Hodgkins[b], N.E. Peters[c]

[a]*Bristol Glaciology Centre, School of Geographical Sciences, University of Bristol, Bristol BS8 1SS, UK*
[b]*Department of Geography, Royal Holloway, University of London, Egham, Surrey TW20 0EX, UK*
[c]*US Geological Survey, 3039 Amwiler Road, 30360-2824 Atlanta, GA, USA*

Abstract

Glacial bulk meltwaters and active-layer groundwaters were sampled from the proglacial zone of Finsterwalderbreen during a single melt season in 1999, in order to determine the geochemical processes that maintain high chemical weathering rates in the proglacial zone of this glacier. Results demonstrate that the principle means of solute acquisition is the weathering of highly reactive moraine and fluvial active-layer sediments by supra-permafrost groundwaters. Active-layer groundwater derives from the thaw of the proglacial snowpack, buried ice and glacial bulk meltwaters. Groundwater evolves by sulphide oxidation and carbonate dissolution. Evaporation- and freeze-concentration of groundwater in summer and winter, respectively produce Mg−Ca-sulphate salts on the proglacial surface. Re-dissolution of these salts in early summer produces groundwaters that are supersaturated with respect to calcite.There is a pronounced spatial pattern to the geochemical evolution of groundwater. Close to the main proglacial channel, active layer sediments are flushed diurnally by bulk meltwaters. Here, Mg−Ca-sulphate deposits become exhausted in the early season and geochemical evolution proceeds by a combination of sulphide oxidation and carbonate dissolution. At greater distances from the channel, the dissolution of Mg−Ca-sulphate salts is a major influence and dilution by the bulk meltwaters is relatively minor. The influence of sulphate salt dissolution decreases during the sampling season, as these salts are exhausted and waters become increasingly routed by subsurface flowpaths.
© 2002 Elsevier Science B.V. All rights reserved.

Keywords: Mg−Ca-sulphate salts; Catchment; Glacier; Proglacial; Chemical weathering; Active layer

1. Introduction

Chemical erosion rates in glacierised catchments are comparable to those in temperate locales with similar specific runoff (Anderson et al., 1997). This is because the colder temperatures and the shorter

rock−water contact times in glacierized catchments, factors which reduce chemical erosion rates, are offset by the abundance of freshly comminuted glacial debris, which are often partially coated with micro-particles (Tranter, 1982). The exposure of geochemically reactive phases, such as carbonates and sulphides (Tranter et al., 1993; Raiswell and Thomas, 1984; Anderson et al., 1997), the lack of inorganic and/or organic coatings (Tranter, 1982), the high proportion of silt-sized debris in moraine (Freeze and

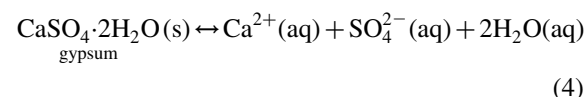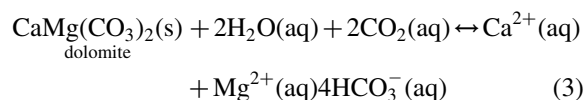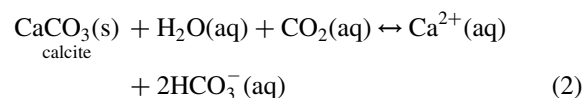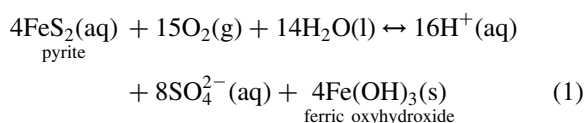* Corresponding author. Tel.: +44-117-9289069; fax: +44-117-9287878.
E-mail address: j.l.wadham@bris.ac.uk (J.L. Wadham).

Cherry, 1979) and the rapid dissolution kinetics of microparticles (Petrovic et al., 1976) enhance the reactivity of glacial debris compared to other types of regolith.

Chemical erosion rates in the region immediately afront the glacier terminus, the 'proglacial zone', have yet to be fully explored, despite preliminary modelling which suggests that this zone may have the potential to significantly perturb concentrations of atmospheric CO_2 (Gibbs and Kump, 1994). The proglacial zone usually comprises a complex mosaic of moraine and glacifluvially reworked sediment and may be seasonally flooded by glacial meltwaters (Wadham et al., 2001). Recent research shows that chemical weathering mechanisms in the proglacial zone are similar to those in subglacial environments (Anderson et al., 2000; Wadham et al., 2001). Sulphide oxidation linked to carbonate dissolution is often a dominant reaction in recently deglacierised moraines and carbonation of silicates becomes increasingly dominant in older moraines as the reactive sulphides and carbonates are exhausted (Anderson et al., 2000).

The only study to date to have derived an annual chemical erosion rate for a proglacial zone was based at Finsterwalderbreen, a High Arctic, polythermal-based glacier on Svalbard (Wadham et al., 2001). Here, proglacial chemical weathering led to a ~30% enhancement of solute flux from the catchment, giving a chemical erosion rate of 2600 mequiv. $\sum^+ m^{-2}$ for the proglacial zone, compared with 790 mequiv. $\sum^+ m^{-2}$ for the glacierized part of the catchment. The purpose of this paper is to describe in detail the hydrochemical processes, by which this high rate of chemical erosion is maintained in the proglacial zone of Finsterwalderbreen. The primary source of solute in this proglacial zone is the chemical weathering of active layer sediments (Wadham et al., 2001), compared to in-channel dissolution of suspended sediment in the glacial bulk meltwaters. We demonstrate that chemical erosion in this permafrost region involves the seasonal precipitation and dissolution of secondary efflorescent salts, particularly gypsum, in the active layer. We focus on three key reactions, the oxidation of sulphides (Eq. (1)), the dissolution and precipitation of carbonates (Eqs. (2) and (3), here described as hydrolysis), and

the precipitation and dissolution of Mg–Ca-sulphate salts such as gypsum (Eq. (4)), and their interactions. Reactions involving silicates have only secondary effects (Wadham et al., 2001).

$$4FeS_2(aq) + 15O_2(g) + 14H_2O(l) \leftrightarrow 16H^+(aq)$$
$$\underset{\text{pyrite}}{} $$

$$+ 8SO_4^{2-}(aq) + \underset{\text{ferric oxyhydroxide}}{4Fe(OH)_3(s)} \tag{1}$$

$$\underset{\text{calcite}}{CaCO_3(s)} + H_2O(aq) + CO_2(aq) \leftrightarrow Ca^{2+}(aq)$$

$$+ 2HCO_3^-(aq) \tag{2}$$

$$\underset{\text{dolomite}}{CaMg(CO_3)_2(s)} + 2H_2O(aq) + 2CO_2(aq) \leftrightarrow Ca^{2+}(aq)$$

$$+ Mg^{2+}(aq)4HCO_3^-(aq) \tag{3}$$

$$\underset{\text{gypsum}}{CaSO_4 \cdot 2H_2O(s)} \leftrightarrow Ca^{2+}(aq) + SO_4^{2-}(aq) + 2H_2O(aq)$$

$$\tag{4}$$

2. Field site description

Finsterwalderbreen (77°28′N, 15°18′E) is a 44 km^2 surge-type glacier located on the southern side of Van Keulenfjorden in southern Svalbard (Fig. 1A). The glacier is over 10 km long, ranges in altitude from 50 to 950 m a.s.l. and occupies a catchment with a total area of 68 km^2 (Hagen et al., 1993). The glacier is polythermal-based, being at the pressure melting point over most of its bed, and has a subglacial drainage system (Hagen et al., 1993). The last surge has been hypothesized to have occurred between 1898 and 1911 (Liestøl, 1969). The proglacial zone covers an area of 4.2 km^2, most of which has only been recently exposed by glacier retreat at a rate of 10–40 m a^{-1} since the termination of the last surge (Nuttall et al., 1997). The proglacial zone is characterised by an outer zone of large terminal moraines and an inner zone of chaotic topography comprising smaller push moraines, a complex network of lakes and an extensive glacifluvial floodplain (Hart and Watts, 1997) (Fig. 1B). The lakes cover ~5% of the proglacial land surface. The thickness of permafrost is estimated to be 200–300 m . The upper layer thaws seasonally to form a shallow active layer. The moraine and fluvio-glacial sediments in the proglacial zone are derived from the local bedrock including Precambrian carbonates, phyllite, and
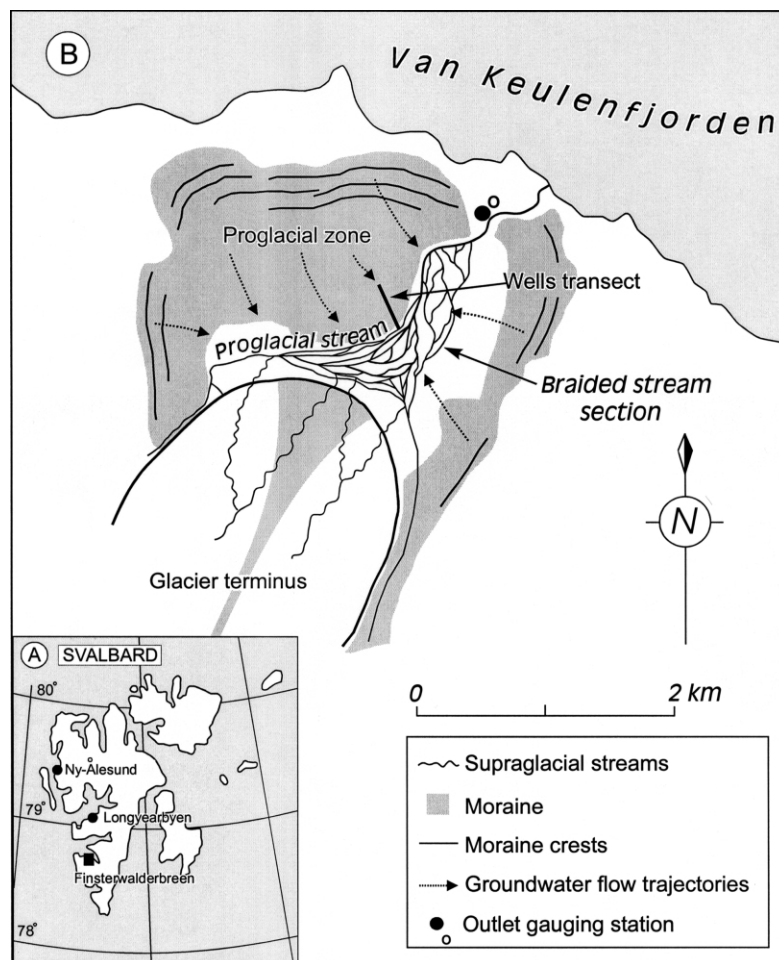
Fig. 1. Location map of (A) Svalbard and (B) the proglacial zone of Finsterwalderbreen.

quartzite, Permian sandstones, dolomites and lime-stones, and Triassic to Cretaceous siltstones, sand-stones and shales (Dallmann et al., 1990). The glacifluvial floodplain is characterised by a braided stream network that conveys glacial bulk meltwaters ca. 2 km downstream from the glacier terminus before forming a single thread channel and discharging into the fjord a short distance downstream (Fig. 1B). Several small streams convey extraglacial runoff, derived from snowmelt, rainfall and in situ thawing of the active layer, along a topographic gradient from the interior of the proglacial moraine system to the glacifluvial floodplain.

3. Methodology

3.1. Field methods

The meltwater sampling reported here was con-ducted from 24th June to 16th August (Days of year, hereafter Days, 175–228) during the 1999 ablation season.

A gauging station was established at the start of the sampling season ~ 2.5 km downstream from the glacier terminus (Fig. 1B). This site, 'the outlet gauging station', was located at the point where the bulk meltwater stream breaches the outer terminal

moraine complex (Fig. 1B), ~ 100 m from where meltwaters enter the fjord. The errors in the discharge were estimated to be ~ 14%.

Stage was measured at 20 s intervals at the outlet gauging station using a Druck pressure transducer. Values were averaged and recorded by a Campbell Scientific CR10X datalogger at hourly intervals. The stage record was calibrated using a stage-discharge rating curve derived from discrete measurements of discharge. Discharge was measured every 4–7 days using the velocity-area wading method (Herschy, 1999). Meltwater samples were collected daily from the bulk meltwater stream that drains the west glacier margin and contributes 70% of the glacial runoff to the proglacial zone.

Three polyvinyl chloride wells were installed in the proglacial active layer along a ~ 120 m transect extending perpendicular to a branch of the main bulk meltwater channel in the middle of the braided stream section (Fig. 1B). Wells 1 and 2 were installed by vertical force and Well 3 was installed by digging a pit in the moraine sediments, installing the well and then back-filling the hole. Wells were 3.9 cm in internal diameter and had five pairs of 0.5 cm × 1 cm horizontal slots cut in the bottom 15 cm. The bottom 20 cm of each well was screened with 257 μm nylon mesh to prevent siltation. The depths of the wells ranged from 0.2 to 0.5 m below the surface of the active layer. Wells 1, 2 and 3 were located 5, 53 and 118 m from the channel, respectively. Wells 1 and 2 were in fine fluvial sediments comprising fine sand and silt on the channel floodplain. Well 2 was adjacent to the moraine fringe. Well 3 was in a poorly sorted gravely sand moraine. The depth of thaw of the active layer adjacent to the channel increased from a mean of 0.40 m at the start of the sampling season in June to 0.75 m in mid August. Water levels and electrical conductivity of waters in wells were monitored every 20 s using DRUCK PDCRl830 pressure transducers and Campbell Scientific combined temperature/conductivity probes, respectively. Both were installed at the base of each well. Hourly averages of readings were recorded by a Campbell Scientific CR10X datalogger. These water level values were converted to hydraulic head values using height data obtained during a field survey of the site.

The saturated hydraulic conductivity (K_{sat}) of the active layer was assessed in the field using failing

head slug tests, which is the standard method for measuring the hydraulic conductivity of sediments surrounding single fully or partially penetrating monitoring wells in unconfined aquifers (Bouwer, 1989). Each test was carried out by recording the time lapse for the water level in a well to return to normal following the addition of ~ 0.5 l of water. Prior to each test, pressure head was monitored at the monitoring well for 10 min to ensure that no significant change in the water table was occurring. During each test, pressure head was logged at 5 s intervals until there was no further change recorded. The hydraulic conductivity of the sediments surrounding the monitoring well was then determined from the Bouwer and Rice (1976) equation,

$$K_{sat} = \frac{R_i^2 \ln(R_r/R_e)}{2L_i} \frac{1}{t} \ln\left(\frac{\psi_0}{\psi_t}\right) \quad (5)$$

where R_i and R_e are the internal and external radii, respectively of the well (m), R_r the effective radial distance over which the increase in pressure head is dissipated (m), L_i the length of the screened intake through which water can enter (m), t is the time since $\Psi = \psi_0(s)$, ψ_0 is the maximum displacement in pressure head at time $t = 0$ (m) and ψ_t is the displacement in pressure head at $t = t$ (m). Since there is no way of knowing what the value of R_r is for a given well, we use the method provided by Bouwer (1989) for estimating the dimensionless ratio ln (R_r/R_e) in partially penetrating monitoring wells (Eq. (6)).

$$\ln\frac{R_r}{R_e} = \left[\frac{1.1}{\ln(L_w/R_e)} + \frac{A + B \ln[(L_b - L_w)/R_e]}{L_i/R_e}\right]^{-1} \quad (6)$$

where, L_w is the distance from the bottom of the well to the water table (m), A and B are dimensionless numbers plotted as a function of L_i/R_e and L_b is the distance from the water table to the bedrock (m), or in this case the upper surface of the permafrost. Values of K_{sat} calculated using this method ranged from 4.4×10^{-5} m s^{-1} in Well 1 to 4.4×10^{-4} m s^{-1} in Well 3. These values fall within the range reported in other studies for moraine and fluvial sediments (Fetter, 1994).

A water sample was collected from each of the wells every four days. Wells were purged of water using a plastic syringe prior to sampling. Water

samples were then drawn from the wells using the syringe, after recharge had occurred. Sample volumes were < 1 casing volume of each well. Recharge typically occurred within 30 s in Well 3 and within 5–10 min in Wells 1 and 2.

The following standard meteorological variables were recorded hourly from Day 113 in 1999 to Day 85 in 2000 using a Campbell Scientific Automatic Weather Station, located 0.75 km north of the glacier terminus within the proglacial moraine complex. Precipitation was measured using a RM Young tipping bucket rain gauge, air temperature, vapour pressure and vapour pressure deficit using a Campbell Scientific HMP 45C relative humidity and temperature probe, wind speed and direction using a RM Young wind monitor, and solar radiation, in the form of global radiation (direct and diffuse), using a Kipp and Zonan SP Lite Pyranometer.

An additional 1 week sampling season was conducted in spring 2000 in order to determine the approximate water equivalents (hereafter w.e.) of snowmelt that accumulate in the proglacial zone over winter. Two snow pits, 0.8 and 1.0 m in depth, were excavated on the glacifluvial floodplain. Snow samples were taken vertically at regular intervals within each pit using a plastic cylinder of known volume. These samples were weighed and used to calculate snow density. Snow depths were measured 3 times at 13 locations throughout the proglacial zone. We appreciate that these measurements will only give an approximation of snow input to the proglacial zone in 1999 since they were conducted the year following the study period. Inter-annual variation in snowfall on Svalbard is typically of the order of $\sim 25\%$, when deduced from mass balance data (Hodson, personal communication).

3.2. Laboratory methods

Groundwater samples were pressure filtered immediately after collection using 0.45 μm cellulose-nitrate membrane filters and a 100 ml plastic syringe and fitted filter head, so as to minimise degassing. Bulk meltwater samples were filtered using 0.45 μm cellulose-nitrate membrane filters, a hand held vacuum pump and a Nalgene filter unit. The filtered samples were sealed in clean low-density polyethylene bottles and stored for 4–6 months prior to

analysis for the major cations, anions, and dissolved Si. pH was determined in the field within several days of collection using an Orion 290 pH meter and a Ross Best Performance pH electrode calibrated using low ionic-strength buffers of pH 4.01, 6.97 and 9.10. The pH of the samples was not significantly affected by storage, because air was largely excluded from the bottles.

Alkalinity (predominantly HCO_3^-) was determined 2 months after collection by colorimetric titration using BDH pH 4.5 indicator. The analytical precision of alkalinity analyses was $\pm 0.1\%$ at HCO_3^- concentrations of 1 mM. Lower analytical precision is anticipated at lower concentrations. For example, a precision of 50% is reported elsewhere for low concentration alkalinity determinations (Tranter et al., 1997). The remaining major cations and anions were determined by ion chromatography on a Dionex 4000i Ion Chromatograph. The analytical precision of ion analyses reported in this paper SO_4^{2-}, Ca^{2+}, Mg^{2+}) was ± 0.9, 0.6 and 0.2%, respectively. Mean charge balance errors (CBEs) (Eq. (7)) calculated for samples collected from the outlet gauging stations and the wells were 2.1 ± 1.8 and $0.5 \pm 3.4\%$, respectively. CBE is defined as,

$$\text{CBE} = \frac{(\sum^+ - \sum^-)}{(\sum^+ + \sum^-)} \times 100\% \qquad (7)$$

where $\sum^-$ and $\sum^+$ are the summed equivalents of the measured anions (NO_3^-, HCO_3^-, SO_4^{2-} and Cl^-) and cations (Na^+, K^+, Ca^{2+} and Mg^{2+}), respectively.

3.3. Data analysis

3.3.1. Evaporation rates

The hourly evaporation rate for the duration of the meteorological monitoring period was calculated using a method for non-saturated surfaces (Granger and Gray, 1989). The general equation employed to calculate the evaporation rate, E, was,

$$E = \frac{\Delta G Q}{(\Delta G + \gamma)} + \frac{\gamma G E_a}{(\Delta G + \gamma)} \qquad (8)$$

where E_a is the drying power of the atmosphere based on well established aerodynamic formulae, Δ the slope of the saturation vapour pressure curve, G is an estimate of relative evaporation (the ratio of actual to potential evaporation) and the relative drying power of the atmosphere (the ratio of

the drying power to the sum of the drying power plus net available energy) (Granger and Gray, 1989). Q is the available energy for evaporation, derived from calculations of net radiation using meteorological data and γ is the psychometric constant. Full details of derivative equations can be found in Granger and Gray (1989).

3.3.2. Groundwater discharge and residence times

Groundwater discharge (GWQ, $m^3 s^{-1}$) was calculated using standard techniques adapted from Freeze and Cherry (1979). The equation employed was,

$$GWQ = (\delta h/\delta l)K_{sat}D_{GW}L_{PG} \tag{9}$$

where, $(\delta h/\delta l)$ is the hydraulic gradient between Wells 1 and 3, calculated using the head difference (δh) and distance between the two wells (δl), and K_{sat} is the saturated hydraulic conductivity of the active layer between these two wells $(m s^{-1})$. D_{GW} is the hourly depth of groundwater in the active layer and L_{PG} is the length of the boundary between the floodplain and moraines. These calculations were performed for every hour during the sampling period. Temporal variation in GWQ is shown in Fig. 2.

Groundwater residence time (GWT) in the ~ 50 m moraine fringe bordering the floodplain (as represented here by the area between Wells 2 and 3)

was calculated by dividing the volume of groundwater in the moraines (GWV) by the hourly groundwater discharge (GWQ). GWV was computed as follows:

$$GWV = {}^mD_{GW}A_{PG}P \tag{10}$$

where, ${}^mD_{GW}$ is the mean hourly depth of groundwater in the active layer, A_{PG} the area of the moraines between Wells 2 and 3 and P is the porosity of the active layer (estimated to be 35% in accordance with typical values for sandy gravel (Fetter, 1994)).

Hourly values of residence time were averaged to give a mean residence time of 459 days for the sampling season. Data for the period Day 199–202, corresponding to a subglacial outburst event, were not included in any of these calculations since there was localised recharge of the active layer at the wells site over this time period. We stress that a mean residence time of 459 is only a crude estimate for several reasons. First, the transect over which these values were calculated included 30 m of floodplain, where the hydraulic gradient was significantly lower. Second, we anticipate that there will be significant variation around this value over the proglacial zone as a whole due to the irregular nature of the topography. Lastly, these calculations do not take account of the fact that in
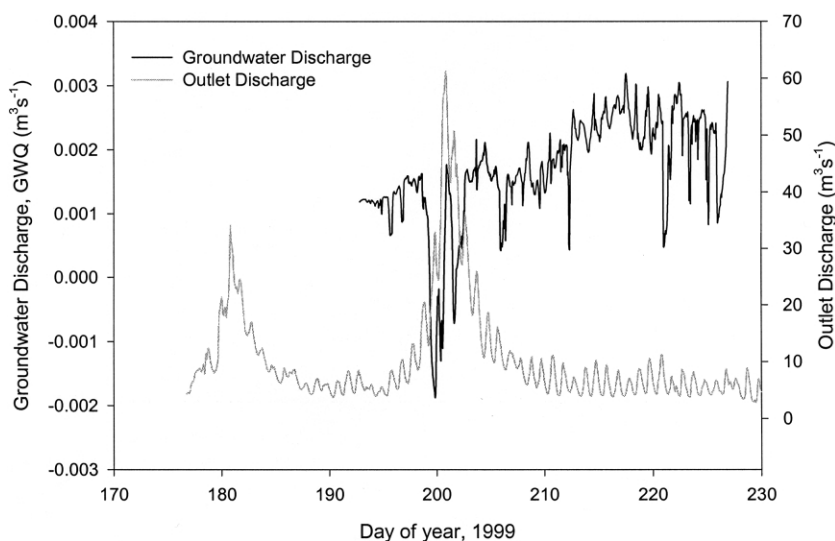

Fig. 2. Temporal variation in groundwater discharge (GWQ) and outlet bulk meltwater discharge during the 1999 sampling season.

many areas, groundwaters drain into surface streams which lower local residence times.

3.3.3. PCO_2 and saturation indices

The partial pressure of CO_2 (PCO_2) of groundwaters and their saturation with respect to calcite (SI_C) and gypsum (SI_{Gyp}) was calculated using PHREEQCI (Parkhurst, 1995). SIs and PCO_2 were calculated at the temperature recorded at the time of sampling, which was typically between 0 and 5 °C.

4. Results

4.1. Hydrology

The seasonal variation in bulk meltwater discharge measured at the outlet during the 1999 sampling season is shown in Fig. 3. The two principal features are maxima on Day 179 and 199, which are associated with the early season snowmelt flood and an outburst of stored subglacial water, respectively. Normally, discharge varied diurnally (with a range of ~ 0.5– $4 \, \text{m}^3 \, \text{s}^{-1}$, equal to a water level change of 0.3–0.7 m) around a daily mean of ~ 3–$5 \, \text{m}^3 \, \text{s}^{-1}$. However, during these flood and outburst events, peak dis-

charges were ~ 30 and $\sim 60 \, \text{m}^3 \, \text{s}^{-1}$, respectively. River stage rose from 0.4 to 1.2 m during these flood events. Bulk meltwaters submerged the near-channel proglacial zone, and promoted a net lateral flow from the channels into the active layer (Figs. 3 and 4). Water levels rose rapidly by ~ 40 cm in the proximal well, Well 1, whereas the distal well, Well 3, showed a more subdued rise of ~ 15 cm, lagged by ~ 6 h. Following the flood, water levels declined, and diurnal variations in water level were clearly discernible in Well 1, whereas in Well 3, these variations were more damped.

The temporal variation in GWQ and discharge at the outlet during the sampling season is shown in Fig. 2. GWQ decreased rapidly to negative values during the subglacial outburst flood, indicating that the active layer was being recharged by channel water. The groundwater flow reversed and discharged to the channel after the channel flow subsided.

4.2. Proglacial hydro-meteorology

Rainfall was the only form of precipitation during the 1999 sampling season and was relatively infrequent, with only 29.4 mm occurring from late June through the middle of August. Rainfall was typically
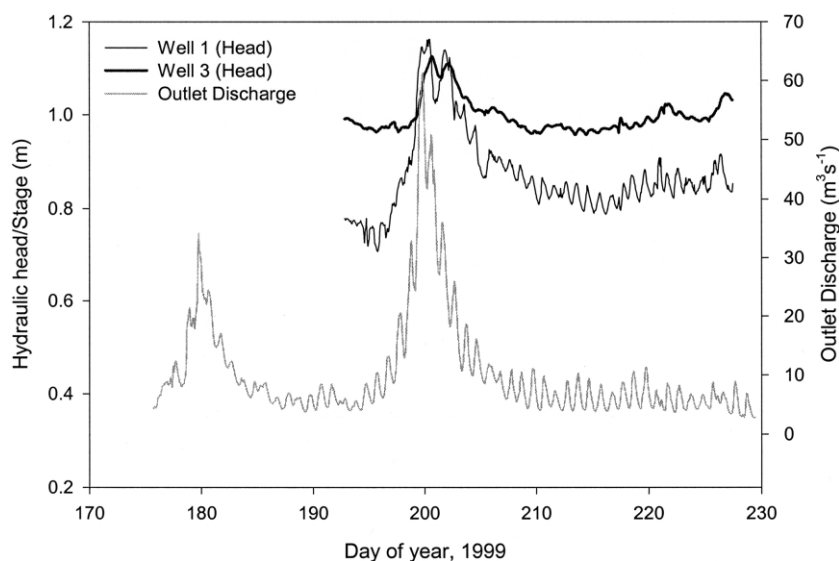

Fig. 3. Temporal variation in outlet bulk meltwater discharge and water levels in Wells 1 and 3 during the 1999 sampling season.
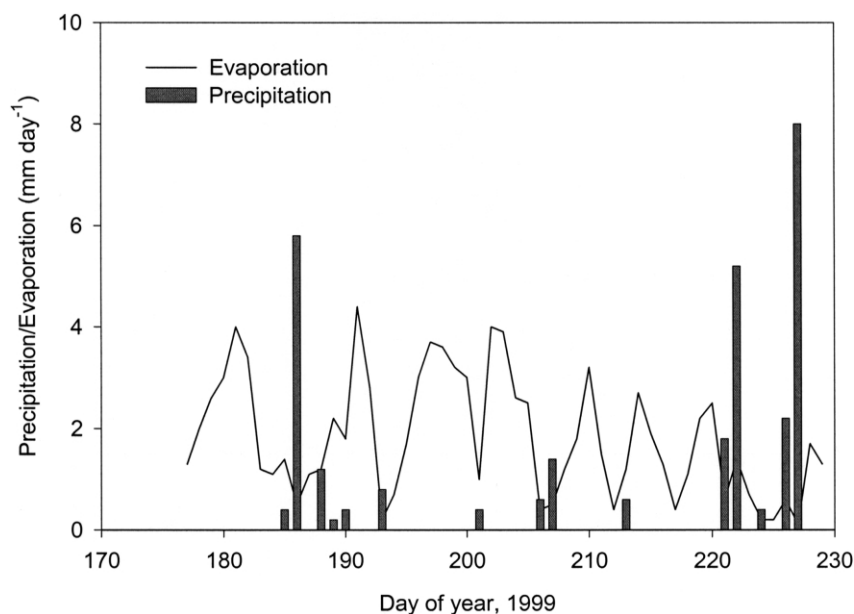
Fig. 4. Temporal variation in evaporation and precipitation in the proglacial zone during the 1999 and sampling season.

associated with the onset of periods of westerly airflow, and spells of significant precipitation were limited to Days 185–190 and 220–227.

The evaporation rate generally decreased throughout the sampling season, ranging from about 1–4 mm d^{-1} during the first half of the season to 0.5–3 mm d^{-1} during the latter half. Periods of relatively high evaporation tended to be associated with relatively high air temperatures and/or strong winds. Notwithstanding the relatively low rates of evaporation, the cumulative evaporation of 196 mm during the 1999 ablation season accounted for ～70% of the total water output from the proglacial zone (see below).

4.3. Proglacial water balance

Although a mean residence time of 459 days suggests that groundwaters reside in the active layer for more than one melt season, our annual observations since 1994 suggest that water inputs to and outputs from the proglacial zone are approximately in balance. This implies that surface runoff plays a major role in delivering water from the interior of the proglacial zone to the main bulk meltwater channel and balancing the hydrological budget. The effective residence time of waters in the proglacial zone may therefore be of the order of a single melt season. Assuming this is the case, it is possible to derive an annual water balance for the proglacial zone using the following equation,

$$P + M + R = GWQ + SQ + E \qquad (11)$$

where P, M and R are water inputs in the form of rainfall, snowmelt and bulk meltwater recharge, respectively, and GWQ, SQ and E are water outputs in the form of groundwater discharge, surface runoff and evaporation, respectively. R was calculated from hourly values of GWQ, which were negative, during the subglacial outburst period. M was calculated by multiplying mean snow depth in the proglacial zone by the mean snow density, both measured in spring 2000. SQ was derived by difference, once the other variables had been calculated. These data are presented in units of mm w.e. in Table 1. Since part of the melt season fell outside of the sampling period, we anticipate that subsurface runoff and rainfall will be underestimated (by <30%) and surface runoff inversely overestimated by a similar quantity. Given

Table 1
Proglacial Water Budget at Finsterwalderbreen for the 1999 sampling season

	Inputs (mm w.e)	Outputs (mm.w.e)
Snowmelt (M)	240	
Rain (P)	29	
Channel Recharge (R)	1	
Evaporation (E)		196
Surface runoff (SQ)		72.5[*]
Subsurface runoff (GWQ)		1.5[**]
Total	270	270

that these components of the water budget were relatively small in magnitude (Table 1), this will have had a minimal effect on the calculations. Evaporation was derived for the entire melt season and has an estimated uncertainty of $\sim +/- 10\%$ arising from errors in the calculation process (Eqs. (7) and (8)).

4.4. Groundwater versus bulk meltwater chemistry

The groundwater and the bulk meltwaters were dominated by Ca^{2+} and SO_4^{2-} and HCO_3^-, with minor amounts of Mg^{2+}. Both Na^+ and Cl^- were in high concentration during snowmelt (Wadham et al., 2001). We confine the following discussion to variations in the Ca^{2+}, Mg^{2+}, SO_4^{2-} and HCO_3^- to focus on the major hydrogeochemical processes in the proglacial zone. Fig. 5 shows the contrasting chemistry of bulk meltwaters, and groundwater from Wells 1, 2 and 3 during the sampling season with respect to the discharge in the channel.

Groundwater HCO_3^- concentrations (Fig. 5) were always higher ($\sim 1500 \mu$equiv. 1^{-1}) than those in the bulk meltwaters ($\sim 500 \mu$equiv. 1^{-1}) and varied systematically during the ablation season. Prior to the outburst, HCO_3^- concentrations in Wells 1 and 3 were similar and those in Well 2 were the most dilute. During the onset of the outburst, groundwater HCO_3^- concentrations increased as floodwater recharged the proglacial zone, but decreased during the recession following the outburst. Thereafter, groundwater HCO_3^- concentrations gradually increased. The increase was greatest in Well 3, where HCO_3^- concentrations exceeded those in Wells 1 and 2.

Ca^{2+} and SO_4^{2-} were higher in the wells (~ 5000

and 4000 μequiv. 1^{-1}, respectively) than the bulk meltwaters (~ 1000 and $\sim 500 \mu$equiv. 1^{-1}, respectively). Well 2 concentrations were always higher than those of Well 1, and were relatively constant. For Wells 1 and 2, the temporal variations in Ca^{2+} and SO_4^{2-} concentrations were similar to those in HCO_3^-. During the onset of the outburst, SO_4^{2-} concentrations decreased slightly in Well 1 and increased in Well 2, whereas the reverse occurred during recession. By contrast, there was more variation in the Ca^{2+} and SO_4^{2-} concentrations of Well 3 (Fig. 6b and c). Well 3 Ca^{2+} and SO_4^{2-} concentrations systematically decreased during the sampling season, from $\sim 13,000$ to $\sim 4000 \mu$equiv. 1^{-1} and $\sim 18,000$ to $\sim 4000 \mu$equiv. 1^{-1}, respectively, with the exception of the last sample collected.

The relation between $(Mg^{2+} + Ca^{2+})$ and SO_4^{2-} is shown in Fig. 6a. There is a strong linear association between these ions for all samples ($p < 0.1$), apart from Well 2. The composition of Well 2 groundwater and the more concentrated Well 3 samples deviates slightly from the linear trend of the bulk meltwaters and Well 1, and lies close to $\sim 1:1$ $SO_4^{2-}/(Mg^{2+} + Ca^{2+})$ relationship. The patterning in the scatterplot of HCO_3^- versus SO_4^{2-} is more complex (Fig. 6b). Well 3 samples largely define a significant negative logarithmic relationship ($p < 1$). Wells 1 and 2 show trends extending from the Well 3 relationship towards the bulk meltwaters. Only the Well 2 relationship is statistically significant ($p < 0.1$). These lineations are evidence for the mixing of bulk meltwaters with groundwater in the near channel sector of the proglacial zone. It is clear, however, that extrapolation of the HCO_3^-/SO_4^{2-} trends in Wells 1 and 2 will be offset from the bulk meltwaters for a similar HCO_3^- concentration. The magnitude of this offset is greater in Well 2 and suggests that there is a variable source of SO_4^{2-} within the sediment of this sector.

All groundwater samples were undersaturated with respect to gypsum. For example, the saturation of groundwaters with respect to gypsum ranged between -1.3 and -1.9 at Well 1, -0.8 and -1.0 at Well 2 and -0.4 and -1.2 at Well 3. In general, the SI_{GYP} decreased as the sampling season progressed. The relationship between the calcite saturation index SI_C and SO_4^{2-} concentration is shown in Fig. 6c. Wells 1 and 2 display weakly positive associations of SO_4^{2-}
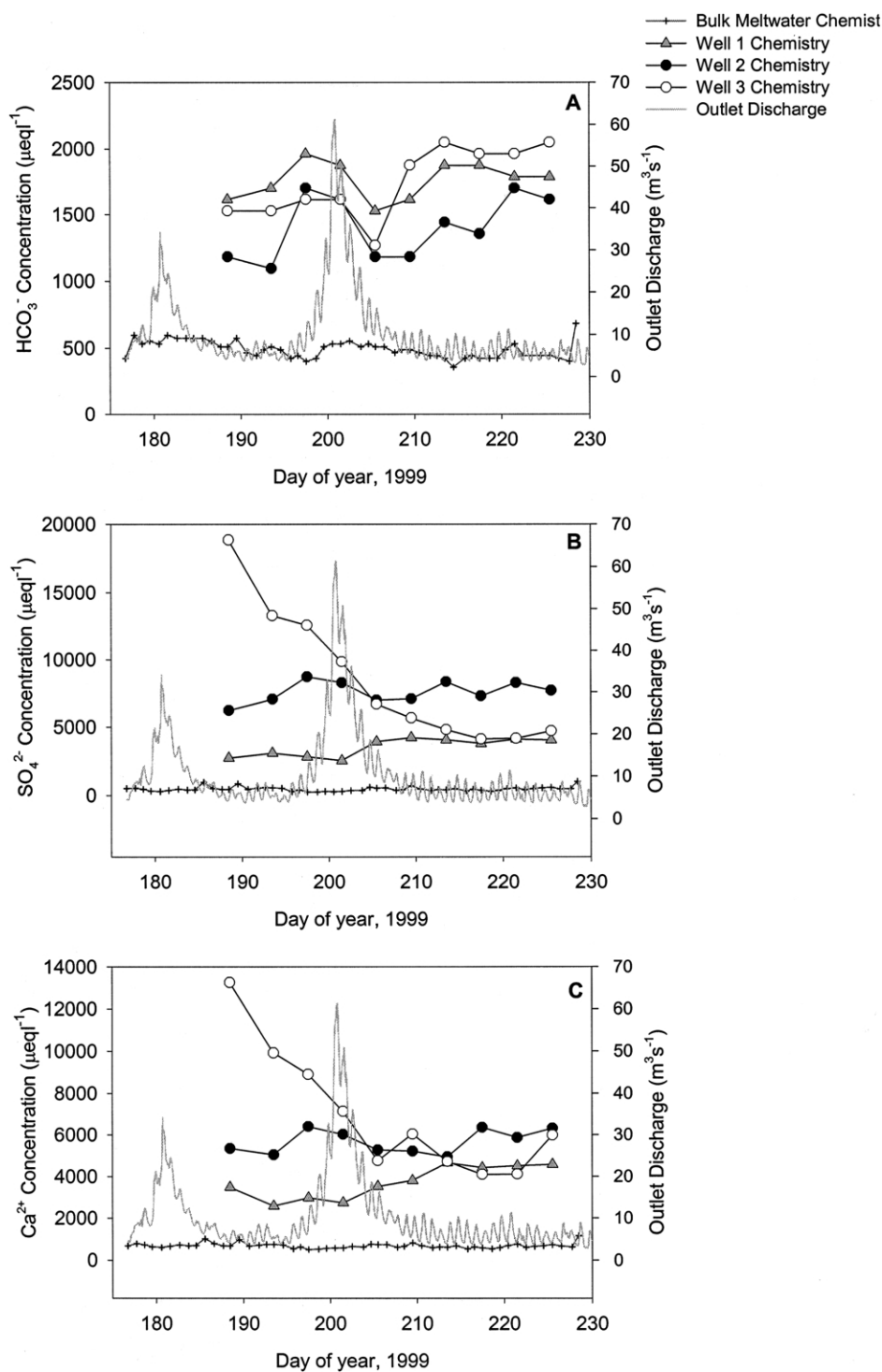
Fig. 5. Temporal variation in the concentrations of (a) HCO_3^-, (b) SO_4^{2-} and (c) Ca^{2+} in Wells 1–3 and the bulk meltwaters during the 1999 sampling season (outlet bulk meltwater discharge is also shown).
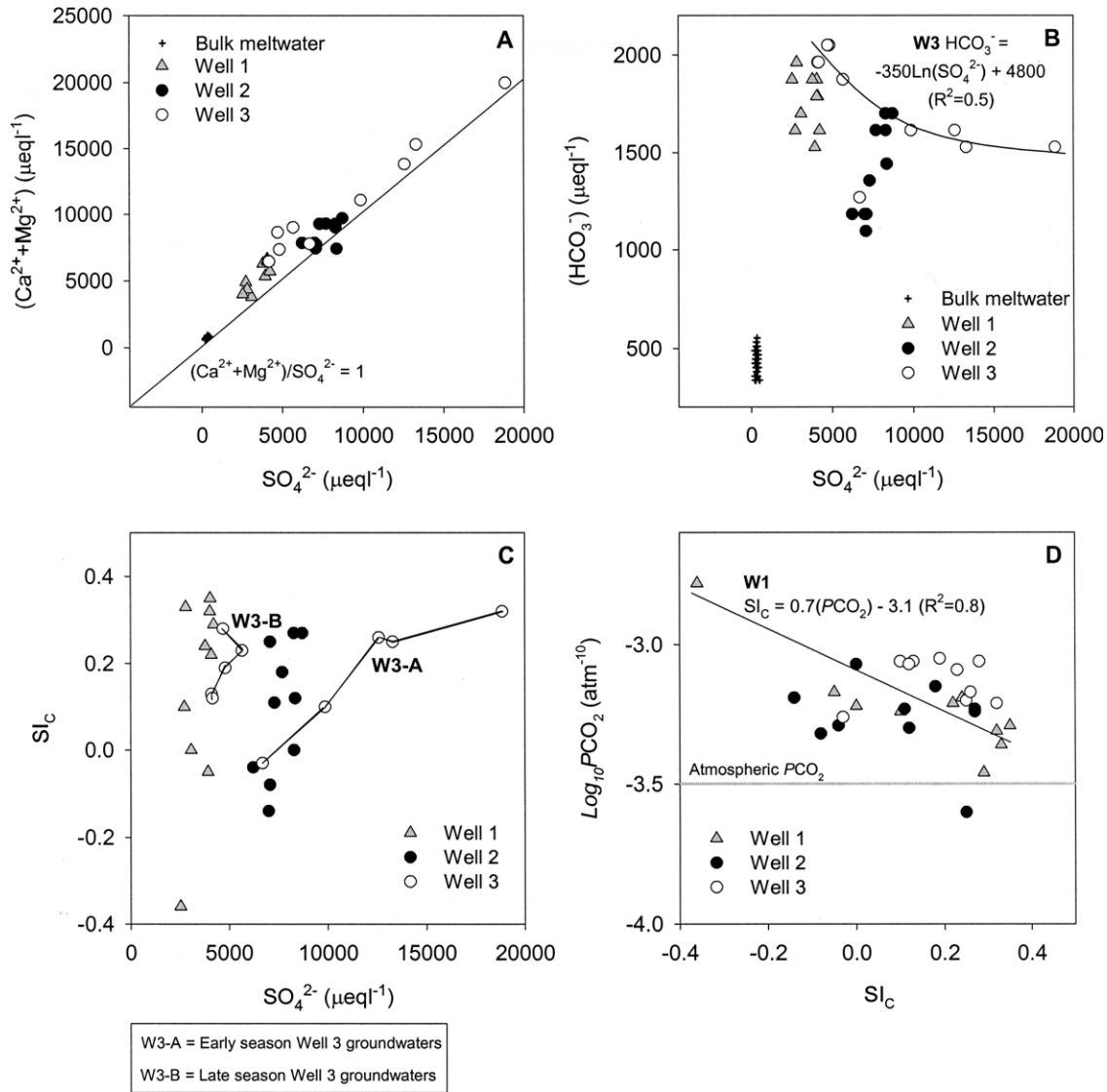
Fig. 6. Associations between (a) $(Ca^{2+} + Mg^{2+})$ and SO_4^{2-} (b) HCO_3^- and SO_4^{2-} (groundwaters and bulk meltwaters) and (c) SO_4^{2-} and SI_C and (d) SI_C and PCO_2 (groundwaters).

and SI_C which are statistically significant ($p < 5$). The relationship for Well 3 is defined by two groups of data points (labelled W3-A and W3-B in Fig. 6). For early season groundwater (W3-A), SI_C significantly decreases with decreasing SO_4^{2-} concentration ($p < 0.1$). For late season groundwater (W3-B), the relation between SI_C and SO_4^{2-} concentration is similar to that for Well 1.

Fig. 6d shows the relationship between the PCO_2 and SI_C of groundwater. Apart from one Well 2 sample, groundwater PCO_2 was greater than atmospheric PCO_2 (-3.5 atm^{-10}). The relationship between PCO_2 and SI_C was only significant for Well 1 ($p < 0.1$), although in this instance it is noted that the strength of the association is highly dependent on one data point. Removal of this point (-0.36 SI_C,

-2.78 PCO_2) gives only a weakly significant relationship ($p < 5$).

5. Discussion

5.1. Hydrology

The main features of the bulk meltwater hydrograph for the 1999 ablation season are the early season snowmelt flood and the mid season outburst flood. The latter event significantly affected water levels in the surface of the glacifluvial floodplain and the adjacent moraines (Fig. 3). Since drainage in both the glacifluvial and moraine sediments is impeded by the presence of the permafrost, recharge resulting from the outburst event was transmitted laterally through the thin active layer. Consequently, water level response times to rising bulk meltwater discharge were rapid, being on the order of $1-2$ h for Well 1 in the glacifluvial sediments adjacent to the stream channel, and $6-12$ h for Well 3 in the moraine sediments bordering the floodplain. Thus, the degree to which water levels in the active layer are coupled to diurnal fluctuations in bulk meltwater discharge decreases with increasing distance from the main channel. The increase in water levels in all wells during the outburst flood is attributable to a large-scale shift in the distribution of the braided bulk meltwater streams from the eastern flank of the floodplain to the western flank. The general increase in water levels in all of the wells late in the season is due to two factors. First, a sustained run of strong easterly winds caused floodplain surface waters to be washed towards the west flank of the floodplain and second, several spells of moderate to heavy rainfall occurred.

Groundwater flow from the moraine sediments to the glacifluvial floodplain was also strongly affected by the outburst event, with the direction being reversed during the period of recharge at the height of the flood. Recharge occurred at a much faster rate than that of post-flood drainage, which took place over 14 days (Fig. 3). Short-lived rapid increases in groundwater discharge late in the season are attributable to the spells of moderate to heavy rainfall mentioned above.

Our observations in the proglacial zone indicate that surface runoff is the most important process delivering groundwater to the proglacial plain during a single melt season, exceeding groundwater discharge almost by an order of magnitude (Table 1). Surface runoff is at a maximum during the thaw at the start of the ablation season, and declines as the ablation season progresses. In contrast, groundwater flow is at a maximum late in the season when the active layer is fully formed. Water levels are very high in the proglacial lakes at the start of the ablation season, having been recharged by local inputs from snowmelt. These lakes typically overflow and are interconnected by a network of ephemeral channels, which together, convey waters to the floodplain. Field observations indicate that most of the proglacial lake network is connected in this fashion at the start of the season. However, as the season progresses and water levels fall, due to progressive evaporative loss and the deepening of the surrounding active layer, these streams dry up and flow is routed below the surface through the sediments of the active layer. The drying of the land surface by drainage and evaporation decreases the rate of evaporation as the season progresses. Evaporative losses represent the greatest output from the proglacial hydrological system (Fig. 4), and exceed rainfall inputs by more than 600%.

5.2. Geochemical processes

High concentrations of HCO_3^- and Ca^{2+} with lower concentrations of Mg^{2+} in active layer groundwater indicate that carbonate, which includes limestone and dolomite, present in proglacial sediments is the rock type being dissolved. The ultimate source of the SO_4^{2-} in these waters must derive from the oxidation of sulphides present in shales and carbonates, because there is no primary gypsum in the underlying bedrock (Dallmann et al., 1990). An important additional source of SO_4^{2-} to groundwater, however, is the dissolution of secondary sulphate salts during summer. These deposits are widespread across the surface of the proglacial zone, being formed by evaporative concentration of groundwater during summer. Some additional sulphate salts may form during winter when freeze concentration of active layer groundwater produces supersaturated conditions. Precipitates collected from the proglacial zone in summer 2000 were dissolved in de-ionised water. The compositions of the resultant leachates are presented in Table 2 and indicate a predominantly $SO_4^2-Mg^{2+}-Ca^{2+}$

Table 2
The chemical composition of efflorescent salts sampled from the surface of the proglacial plain, when 2 g samples were dissolved in 50 ml deionised water and left for 12 h prior to filtering for chemical analysis (Farmer, personal communication)

	$(Ca^{2+} + Mg^{2+})/SO_4^{2-}$	Concentration (μeql^{-1})			
		Mg^{2+}	Ca^{2+}	HCO_3^-	SO_4^{2-}
Sample 1	0.95	49,000	15,000	1,800	65,000
Sample 2	0.96	1,500	29,000	1,800	30,000
Sample 3	0.94	28,000	17,000	2,700	45,000
Sample 4	0.96	0	24,000	1,000	24,000
Mean	0.95	20,000	22,000	1,800	46,000

composition. Samples 2 and 4 are dominated by Ca^{2+} and SO_4^{2-} and indicate that some proglacial efflorescent salts constitute pure gypsum.

The hydrochemical trends observed in the three wells can be explained by four geochemical processes: (1) sulphide oxidation, (2) carbonate dissolution, (3) precipitation of calcite and Mg–Ca-sulphate salts, and (4) dissolution of the secondary calcite and sulphate salts during the melt season. The relative dominance of these geochemical processes in controlling groundwater evolution is determined, in part, by well proximity to the bulk meltwater channel and the hydraulic transmissivity of the active layer sediments which affects the flushing of the active layer by channel meltwaters.

Water levels in Well 1 are strongly coupled to bulk meltwater discharge variations (Fig. 3). Daily and episodic mixing between this groundwater and dilute bulk meltwaters produces the linear trends in $(Ca^{2+} + Mg^{2+})$ versus SO_4^{2-} and HCO_3^- versus SO_4^{2-}. The associations approximately align with the corresponding bulk meltwater relationships (Fig. 6). The relatively small offset from the bulk meltwater HCO_3^- versus SO_4^{2-} relationship suggests that mixing in this channel marginal zone is more conservative than at greater distances from the channel (see below). The slope of the $(Ca^{2+} + Mg^{2+})$ versus SO_4^{2-} relationship is >1:1 and aligns more closely with that displayed by the bulk meltwaters than with the two other wells, indicating that sulphate salt dissolution is probably not as dominant a process in Well 1 waters. Given the proximal position of this well relative to the bulk meltwaters, any sulphate salts would be removed as soon as the bulk meltwater stream inundates these sediments (during the spring snowmelt flood. Formation of efflorescent Mg–Ca-

sulphate salts here is unlikely given the diurnal flushing of the fluvial sediments by bulk meltwaters.

For the transect studied, the hydrochemical influence of the bulk meltwater stream should be the smallest in Well 3, where there is a 6–12 h lag between discharge variations and water level response (Fig. 3). Correspondingly, the HCO_3^-/SO_4^{2-} and $(Ca^{2+} + Mg^{2+})/SO_4^{2-}$ relationships for the Well 3 groundwater are not suggestive of mixing with bulk meltwaters (Fig. 6), although the water level fluctuates daily. This implies that input waters constitute either bulk meltwaters that have rapidly acquired solute during transit through the intervening proglacial sediments or, more likely, concentrated groundwater that has evolved in situ and been displaced from more proximal channel settings by the incoming bulk meltwaters. Electrical conductivity measurements showed no significant variation with water level in Well 3 and are consistent with these hypotheses. The chemistry of Well 3 groundwater clearly indicates the dissolution of sulphate salts. Ratios of $(Ca^{2+} + Mg^{2+})/SO_4^{2-}$ are close to 1:1 (Fig. 6) and similar to those found in proglacial salt leachates (Table 1), which is consistent with the hypothesis that the dissolution of these salts is important to the evolution of groundwater quality. Well 3 waters display strong seasonal trends in composition that arise from the exhaustion of Mg–Ca-sulphate salts. First, SO_4^{2-} and Ca^{2+} concentrations decrease during the sampling season (Fig. 5). Second, the $(Ca^{2+} + Mg^{2+})/SO_4^{2-}$, and HCO_3^-/SO_4^{2-} ratios evolve towards those displayed by Well 1 (Fig. 6), where daily flushing by the bulk meltwaters results in the early removal of all surficial Mg–Ca-sulphate salts. Third, the lack of a significant relationship between PCO_2 and SI_C (Fig. 6d) suggests that

degassing of CO_2 is not a first order control on the SI_C. Fourth, a significant positive relationship between SO_4^{2-} and SI_C in Well 3 waters during the early season (Fig. 6c) indicates that the dissolution of the Mg–Ca-sulphate salts primarily controls the SI_C, such that the associated addition of SO_4^{2-} and Ca^{2+} to groundwater increases the SI_C by the common ion effect.

The progressive decline in Well 3 SO_4^{2-} concentrations during the sampling season and decrease in SI_C may account for the corresponding increase in HCO_3^- as more calcite dissolves Plummer and Busenberg, 1982). The pH over this time period is quasi-constant so cannot explain the decrease in SI_C. Hence, loss of Ca^{2+} by sulphate salt dissolution through the season is compensated by enhanced acquisition of Ca^{2+} and HCO_3^- from carbonate dissolution (Fig. 5).

The chemical evolution of Well 2 groundwater, which lies in the middle of the well transect, reflects the combined effects of bulk meltwater recharge, groundwater recharge, and in situ weathering. Dilution during bulk meltwater recharge is evident from the linear trends of HCO_3^-/SO_4^{2-} and $(Ca^{2+} + Mg^{2+})/SO_4^{2-}$ (Fig. 6). The 2000 μequiv. l^{-1} offset of the HCO_3^-/SO_4^{2-} lineation from the extrapolated bulk meltwater composition suggests that there is a supply of additional SO_4^{2-} and that mixing with channel waters is less conservative than in Well 1. The source of the excess SO_4^{2-} is probably both sulphide oxidation and Mg–Ca-sulphate salt dissolution. Again the 1:1 relationship of $(Ca^{2+} + Mg^{2+})/SO_4^{2-}$ is consistent with this (Fig. 6a). Salt derived SO_4^{2-} may not necessarily be generated in situ but may be advected from neighbouring moraines during recharge.

Geochemical processes in the proglacial active layer are strongly seasonal and the seasonality varies spatially. Seasonal patterns are most clearly evident in the progressive exhaustion of Mg–Ca-sulphate deposits, which may be formed at depth in the active layer by freeze concentration during winter and occur on the surface by evaporative concentration in summer. Most of the latter efflorescent salts are believed to re-dissolve either later in the same summer during rain events or the following year during snowmelt, when the active layer is thin and surface runoff dominates. Spatial patterns in groundwater geochemistry primarily reflect proximity to the bulk meltwater stream, with the extent of groundwater dilution decreasing with increased distance from the main channel.

The hydrology of the proglacial zone is key to the acquisition of solute by the bulk meltwater during transit through the proglacial plain and the consequent augmentation of solute fluxes at Finsterwalderbreen (Wadham et al., 2001). An extensive active layer containing reactive elements and irregular topography means that snowmelt and rainfall are stored for a prolonged time period. A complex network of lakes and surface streams enables these meltwaters to be evacuated from the proglacial zone over the melt season and delivered via a topographic gradient to the floodplain. Solute is also added to the bulk meltwaters during periods of high discharge when the channel expands over its floodplain and there is mixing between in situ groundwaters and bulk meltwaters. These findings contrast with results presented in some other proglacial geochemistry studies (Fairchild et al., 1999), where a smaller groundwater reservoir and relatively poor hydrological connections between this reservoir and the bulk meltwater channel mean that proglacial chemical weathering is much less effective.

6. Conclusions

High rates of chemical weathering in the proglacial zone of Finsterwalderbreen are explained primarily by prolonged chemical weathering of highly reactive debris held in fluvial and moraine deposits of the proglacial active layer. Chemical evolution of active layer groundwater proceeds by a combination of sulphide oxidation, carbonate dissolution, Mg–Ca-sulphate salt and calcite precipitation and subsequent re-dissolution of these precipitates.

Spatial patterns in geochemical evolution exist and reflect the varying influence of the bulk meltwater channel on active layer hydrology. Fluvial active layer sediments close to the channel margins are flooded on a daily basis during the melt season. The chemical composition of groundwater shows no evidence of sulphate salt precipitation and evolves by coupled carbonate dissolution/sulphide oxidation. Dilution trends in the chemistry are evidence of close

exchange of water with the main channel. Degassing of CO_2 mainly controls the saturation of the proglacial zone groundwater with respect to calcite.

The moraine interior, located > 100 m from the channel exhibits no dilution by bulk meltwaters. The dissolution of efflorescent sulphate salts, formed by freeze concentration in winter and evapo-concentration in summer, dominates groundwater hydrochemistry at the start of the melt season and high SI_C values are maintained by the common ion effect. Mg–Ca-sulphate salts are exhausted during the sampling season in distal locations, and groundwater chemistry trends towards that observed in more proximal settings, where sulphide oxidation and carbonate dissolution are the first order processes.

Active layer groundwater located in intermediate locations evolves by carbonate dissolution/sulphide oxidation, together with some dissolution of Mg–Ca-sulphate salts. Solute is exported from the proglacial zone by the bulk meltwater stream. A complex network of interconnected lakes is responsible for conveying meltwaters along a topographic gradient to the proglacial floodplain and into the bulk meltwater channel. Some solute also is mobilised directly by the bulk meltwaters during subglacial flood events, when the channel expands into the adjacent fluvial floodplain sediments.

Several factors facilitate high rates of chemical erosion in the proglacial zone of Finsterwalderbreen. First, moraines and fluvial deposits contain an abundance of reactive formerly subglacial debris generated originally by comminution at the temperate glacier sole. Second, a network of lakes and streams is able to both store snowmelt in the early melt season and ensure a ready supply of meltwater to the active layer. Finally, a dynamic glacial meltwater flux through the proglacial zone means that proximal active layer sediments are periodically flooded and recharged with dilute meltwaters.

References

Anderson, S.P., Drever, J.I., Humphrey, N.F., 1997. Chemical weathering in glacial environments. Geology 25, 399–402.

Anderson, S.P., Drever, J.I., Frost, C.D., Holden, P., 2000. Chemical weathering in the foreland of a retreating glacier. Geochim. Cosmochim. Acta 64 (7), 1173–1189.

Bouwer, H., 1989. The Bouwer and Rice slug test—an update. Groundwater 27 (3), 304–309.

Bouwer, H., Rice, R.C., 1976. A slug test for determining hydraulic conductivity of unconfined aquifers with completely or partially penetrating wells. Water Resour. Res. 12, 423–428.

Dallmann, W.K., Hjelle, A., Ohta, Y., Salvigsen, O., Bjornerud, M.G., Hauser, E.C., Maher, H.D., Craddock, C., 1990. Geological map, Svalbard, Van Keulenfjorden B11G, Norsk Polarinstitutt, Oslo.

Fairchild, I.J., Killawee, J.A., Sharp, M.J., Hubbard, B., Lorrain, R.D., Tison, J.L, 1999. Solute generation and transfer from a chemically reactive alpine glacial-proglacial stem. Earth Surf. Process. Landforms 4 (13), 1189–1211.

Fetter, C.W., 1994. Applied Hydrogeology, Prentice Hall, New Jersey.

Freeze, R.A., Cherry, J.A., 1979. Groundwater, Prentice Hall, New Jersey.

Gibbs, M.T., Kump, L.R., 1994. Global chemical erosion during the last glacial maximum and the present: sensitivity to changes in lithology and hydrology. Paleoceanography 9, 529–543.

Granger, R.J., Gray, D.M., 1989. Evaporation from natural nonsaturated surfaces. J. Hydrol. 111, 21–29.

Hagen, J.O., Liestøl, O., Roland, E., Jørgensen, T., 1993. Glacier Atlas of Svalbard and Jan Mayan, vol. 129. Norsk Polarinstitutt Meddelser.

Hart, J.K., Watts, R.J., 1997. A comparison of the styles of deformation associated with two recent push moraines, south Van Keulenfjorden, Svalbard. Earth Surf. Process. Landforms 22, 1089–1107.

Herschy, R.W., 1999. Hydrometry. Principles and Practices, Second ed, Wiley, Chichester.

Liestøl, O., 1969. Glacier surges in West Spitsbergen. Can. J. Earth Sci. 6, 895–897.

Nuttall, A.M., Hagen, J.O., Dowdeswell, J.A., 1997. Quiescent-phase changes in velocity and geometry of Finsterwalderbreen, a surge-type glacier in Svalbard. Ann. Glaciol. 24, 249–254.

Parkhurst, D.L., 1995. User's guide to PHREEQC—a computer program for speciation, reaction-path, advective-transport, and inverse geochemical calculations. US Geological Survey Water-Resources Investigations Report 95-4227, 143 pp.

Petrovic, R., Berner, R.A., Goldhaber, M.B., 1976. Rate control in dissolution of alkali feldspars I. Study of residual grains by X-ray photoelectron spectroscopy. Geochim. Cosmochim. Acta 40, 537–548.

Plummer, L.N., Busenberg, E., 1982. The solubilities of calcite, aragonite and vaterite in CO_2–H_2O solutions between 0 and 90 °C, and an evaluation of the aqueous model for the system $CaCO_3$–CO_2–H_2O. Geochim. Cosmochim. Acta 46, 1011–1040.

Raiswell, R., Thomas, A.G., 1984. Solute acquisition in glacial meltwaters I. Fjällsjökull (south-east Iceland): bulk meltwaters with closed system characterist. J. Glaciol. 30 (104), 35–43.

Tranter, M., 1982. Controls on the chemical composition of Alpine glacial meltwaters. PhD Thesis, University of East Anglia.

Tranter, M., Brown, G.H., Raiswell, R., Sharp, M.J., Gurnell, A.M., 1993. A conceptual model of solute acquisition by Alpine glacial meltwaters. J. Glaciol. 39 (133), 573–581.

Tranter, M., Sharp, M.J., Brown, G.H., Willis, I.C., Hubbard, B.P., Nielsen, M.K., Smart, C.C., Gordon, S., Tulley, M., Lamb, H.R., 1997. Variability in the chemical composition of in situ subglacial meltwaters. Hydrol. Process. 11, 59–77.

Wadham, J.L., Cooper, R.J., Tranter, M., Hodgkins, R., 2001. Enhancement of glacial solute fluxes in the proglacial zone of a polythermal glacier. J. Glaciol. 47 (157), 378–386.